

# A Numerical Study of Different Metal and Prism Choices in the Surface Plasmon Resonance Biosensor Chip for Human Blood Group Identification

Sanjeev Kumar Raghuwanshi<sup>ID</sup>, Senior Member, IEEE,  
and Purnendu Shekhar Pandey<sup>ID</sup>, Graduate Student Member, IEEE

**Abstract**— Optimized design of Surface plasmon resonance (SPR) based biosensor in terms of different metal choices and prisms are presented to the first time for the high precision detection of human blood group in near infrared wavelength range. The results are well compared with the earlier published gold coated silicon biosensor chip while discussing the pros and cons of various prism/metal choices. In this study buffer layer onto SPR active metal has been deployed to avoid the oxidation problem and contamination issue related with blood samples. Refractive index of blood samples has been considered in theoretical model based on the experimental data. Si prism has been found to be the best choice as a substrate material with combination of Al as a SPR active metal for blood group identification analysis. SPR dip slope (S), detection accuracy (D.A.) and blood group discrimination factor ( $\delta\theta_{SPR}$ ) have been studied with respect to different metal choices with their suitability to the next generation biosensor applications.

**Index Terms**— Blood groups, SPR Sensor, biosensor, detection accuracy (D.A.), FWHM, sensitivity slope, SPR dip, wavevector, transfer matrix method (TMM) etc.

## I. INTRODUCTION

SURFACE plasmon resonance (SPR) has been proved to be very potential candidates to the next generation sensing technology specially related to biosensor domain. To generate the SPR the glass prism is coated by thin metal film followed by analytes. SPR phenomena is related with collective oscillation of electrons at metal/dielectric interface in controlled manner by the incident of p-polarized light at the boundary of

Manuscript received 14 May 2022; revised 6 June 2022; accepted 19 June 2022. Date of publication 23 June 2022; date of current version 3 April 2023. This work was supported in part by the Design and development of deployable thin film based evanescent field sensor to check the quality of food from adulteration through the Council of Scientific and Industrial Research (CSIR), New Delhi, Government of India under Sanction 70(0077)/19/EMR-II [IIT(ISM) and Project CSIR(32)/2019-2020/663/ECE] and in part by CSIR-Central Scientific Instruments Organisation (CSIO), Chandigarh, India. (Corresponding author: Sanjeev Kumar Raghuwanshi.)

The authors are with the Department of Electronics Engineering, Indian Institute of Technology (Indian School of Mines) Dhanbad, Jharkhand 826004, India (e-mail: sanjeevrus77@iitism.ac.in).

Digital Object Identifier 10.1109/TNB.2022.3185806

two different medium. Plasmon has to excite at optimum thickness of metal film, certain wavelength and precise condition of launching angle to the first incident medium. Plasmonic oscillations are occurred only when free electrons of metal coherently interact with light or photon on an interface of dielectric and metal. This is called SPR condition and satisfied at particular incident angle for a given wavelength and metal thickness. Evanescent field penetrates much deeper to the substance or analyte layer only when SPR condition is satisfied. If  $n_s(\lambda)$  is the wavelength dependent refractive index of analyte or substance,  $n_p(\lambda)$  is the wavelength dependent refractive index of light coupling prism or substrate material,  $\epsilon_M(\lambda)$  is the wavelength dependent dielectric constant of the metal and wavelength of incident light  $\lambda$ , then SPR condition is satisfied by the following equation [1], [2]:

$$k_0 n_p(\lambda) \sin(\theta_i) = k_0 R e \left( \sqrt{\frac{\epsilon_M(\lambda) n_s(\lambda)^2}{\epsilon_M(\lambda) + n_s^2(\lambda)}} \right) \quad (1)$$

where  $k_0 = \frac{2\pi}{\lambda}$ . The right hand side term of the eq. (1) is surface plasmon wave propagation constant  $K_{SPR}(\lambda)$  and left hand side is the propagation constant of incident wave  $K_{incident}(\lambda)$  at an angle  $\theta_i$  of incident light beam through a light coupling prism of refractive index  $n_p(\lambda)$ . SPR condition  $K_{incident}(\lambda)|_{\lambda=\lambda_{fix}} = K_{SPR}(\lambda)|_{\lambda=\lambda_{fix}}$  would be satisfied at  $\theta_i = \theta_{SPR}$ . The reflected power has a sharp dip at  $\theta_i = \theta_{SPR}$  called to be SPR dip. This SPR dip “ $\theta_{SPR}$ ” is highly susceptible to change of analyte or outer medium refractive index. Sensitivity of SPR sensor is defined by the shift of SPR resonance angle ( $\delta\theta_{SPR}$ ) with respect to shift of sensing layer refractive index  $\delta n_s(\lambda)$ . Indeed sensitivity would be maximum for a substantial shift of SPR resonance angle for a minute change of sensing layer refractive index. Another important performance parameter of SPR sensing chip is full width at half maximum (FWHM), which decides the detection accuracy (D.A.) of sensing chip. FWHM should be as small as possible so that the error in detection of SPR dip can be minimized. It means D.A. of SPR sensor is inversely proportional to the FWHM of SPR curve. Fig. 1(a) shows the

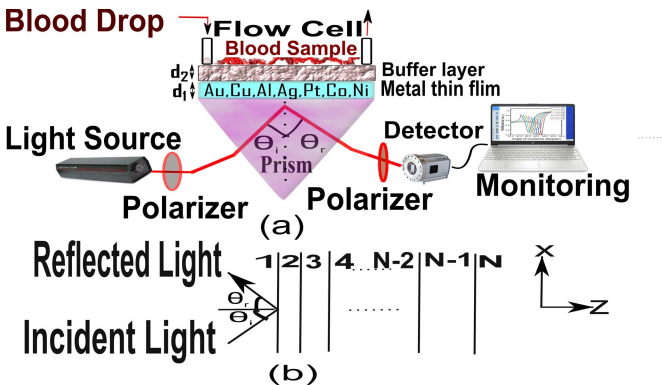


**Fig. 1.** a) Schematic diagram of the proposed glass prism based SPR biosensor with different metallic choices for identification of different human blood groups. b) Layers in TMM method are assumed to be stacked along z-direction.

proposed kretschmann configuration sensing system which is one of the most prominent configuration among SPR scientific community. In this configuration thin metal film of few tens of nanometer can be directly deposited on substrate prism either by thermal or electron beam evaporation system. To couple the light effectively in kretschmann configuration the refractive index of substrate material prism  $n_P$  should be greater than that of sensing medium  $n_s$ .

High refractive index prism is required to effectively coupled the light with outer most layer of sensing chip hence the choice of prism is an important criterion to achieve the high precision in sensing of blood group. It is important to mention here that apart of that, choices of metals are again challenging issues for their better performance parameters like figure of merit (FOM), detection accuracy (D.A.), full width at half maximum (FWHM) and sensitivity slope (S). In this paper Cu, Al, Ag, Au, Pt, Co and Ni metals are considered into theoretical modelling of prism based SPR sensor. SPR phenomena based on prism or glass substrate coated by thin metal layer is widely used in recent past for bio-sensing applications. The sensitivity of blood group detection along with proper analytical modelling of SPR excitation phenomena are presented by using transfer matrix method (TMM) [2]–[11]. Li. *et al.* [5] developed a Cauchy formula based on their experimental results for the dispersion or refractive index relation of three blood samples as follow

$$n_s(\lambda)|_i = 1.357 + \frac{K_1}{\lambda^2} + \frac{K_2}{\lambda^4} \quad (2)$$

where  $\lambda$  is in nm, also subscript  $i$  in eq. (2) stands for  $i=O$ ,  $i=B$  and  $i=A$  to blood samples “O”, “B” and “A” respectively. Infact  $n_s(\lambda)|_i = n_s(\lambda)$  while comparing with eq. (1) for single analyte sample. Cauchy coefficients  $K_1$  and  $K_2$  have distinct values for different blood groups. Fig.2 reveals the graph for different blood groups corresponding to eq. (2) and these data has been used in this paper [5]. In recent past SPR sensor has been successfully demonstrated to detect several biological parameters like DNA, proteins, pesticides, immunoassays to name a few [1]. Recently several authors worked on blood group identification of human beings but optimization with respect to SPR active metal and prism is still missing as per the

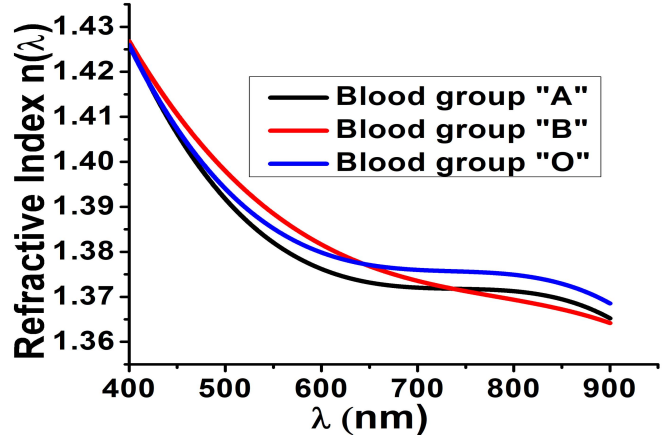


**Fig. 2.** Accurate variation of three different blood groups versus wavelength (data available in  $400\text{nm} \leq \lambda \leq 900\text{nm}$  range) for  $C_A = 150.2\text{g/L}$ ,  $C_B = 140.4\text{g/L}$  and  $C_O = 135.33\text{g/L}$  are blood group concentration of “A”, “B” and “O” respectively [5]–[7] at room temperature  $25^\circ\text{C}$ .

authors knowledge. Hence, in this paper the choice of metals and prisms for high sensitivity detection are reported for the first time.

## II. THEORETICAL MODELING AND DESIGN CONSIDERATIONS OF SPR SENSOR

In Fig. 1 prism (e.g., Si, BK7, SF11, 2S2G, LINBO<sub>3</sub> and SiO<sub>2</sub>) is coated by thin SPR active metal film (Cu, Al, Ag, Au, Pt, Co and Ni) of  $d_1 = 50$  nm thickness either by thermal or e-beam evaporation technique. Here choice of prism and metal is an important criteria to achieve the highest optimum performance parameters e.g. shift of SPR resonance dip for different blood groups. In this paper various types of prism based on Silicon (Si), BK7, SF11, 2S2G, LINBO<sub>3</sub> and SiO<sub>2</sub> (silica) are considered for better clarity of choice of silicon as a substrate material [1], [3], [10], [12]–[14]. However, the actual application of chosen prism for particular sensor design parameters are crucial task and need the further investigations. Refractive index variation of Silicon (Si) prism with wavelength is expressed by

$$n_P(\lambda) = 3.5 + 2271.9e^{-\frac{\lambda}{0.05304}} + 3.4e^{-\frac{\lambda}{0.30384}} \quad (3)$$

The refractive index variation of LINBO<sub>3</sub> prism is expressed by

$$n_P(\lambda) = \sqrt{1 + \frac{2.67\lambda^2}{\lambda^2 - 0.018} + \frac{1.3\lambda^2}{\lambda^2 - 0.06} + \frac{12.6\lambda^2}{\lambda^2 - 474.6}} \quad (4)$$

The refractive index of BK7 prism is expressed by

$$n_P(\lambda) = \sqrt{1 + \frac{1.0397\lambda^2}{\lambda^2 - 0.006} + \frac{0.2318\lambda^2}{\lambda^2 - 0.02} + \frac{1.0105\lambda^2}{\lambda^2 - 103.56}} \quad (5)$$

The refractive index of SF11 prism is expressed by

$$n_P(\lambda) = \sqrt{1 + \frac{1.74\lambda^2}{\lambda^2 - 0.013} + \frac{0.313\lambda^2}{\lambda^2 - 0.063} + \frac{1.8987\lambda^2}{\lambda^2 - 155.3}} \quad (6)$$

TABLE I  
METAL DIELECTRIC CONSTANTS [16], [17]

Serial no.	Metal	$\lambda_p$ ( $\mu\text{m}$ )	$\lambda_c$ ( $\mu\text{m}$ )
1	Au	0.16826	8.9342
2	Ag	0.14541	17.614
3	Cu	0.13617	40.852
4	Al	0.10657	24.511
5	Pt	0.2415	17.95
6	Co	0.31215	33.578
7	Ni	0.25381	28.409

The refractive index of fused silica ( $\text{SiO}_2$ ) with wavelength is determined by the Sellmeier relation as follow

$$n_P(\lambda) = \sqrt{1 + \frac{a_1\lambda^2}{\lambda^2 - b_1^2} + \frac{a_2\lambda^2}{\lambda^2 - b_2^2} + \frac{a_3\lambda^2}{\lambda^2 - b_3^2}} \quad (7)$$

where  $a_1 = 0.6961662$ ,  $a_2 = 0.4079426$ ,  $a_3 = 0.8974794$ ,  $b_1 = 0.0684043$ ,  $b_2 = 0.1162414$  and  $b_3 = 9.896161$  are the Sellmeier coefficients of fused silica glass. The wavelength dependence of the refractive index of the Chalcogenide (2S2G) prism is given by

$$n_P(\lambda) = 2.2407 + \frac{0.02693}{\lambda^2} + \frac{0.00808}{\lambda^4} \quad (8)$$

where, wavelength of incident light  $\lambda$  is measured in  $\mu\text{m}$  in all above eq. (3-8). Infact Si and 2S2G prisms have a high refractive index as compared to silica, BK7, SF11 and  $\text{LiNbO}_3$  based prism under consideration in this work. However Si win the race even with 2S2G, which is quite advantageous for coupling the light from the prism to the surrounding layers and substances. It opens the new window of sensing applications in infrared (IR) band, further brief discussion about the selection of prism is discussed in next section of this paper. The free electron Drude model has been used to express the complex refractive index of various metals under consideration in this work as follow [2]

$$\tilde{n}_m(\lambda) = \sqrt{\tilde{\epsilon}_m(\lambda)} = \sqrt{1 - \frac{\lambda^2\lambda_c}{\lambda_p^2(\lambda_c + i\lambda)}} \quad (9)$$

where  $\lambda_p$  and  $\lambda_c$  is the plasma and the collision wavelengths of various metals as listed in Table-I [15] and  $\lambda$  is measured in  $\mu\text{m}$ . It is assumed that  $\tilde{n}_m = n + ik$  and  $\tilde{\epsilon}_m = \epsilon_1 + i\epsilon_2$ , where wavelength dependency of  $\tilde{n}_m$ ,  $\tilde{\epsilon}_m$ ,  $n$ ,  $k$ ,  $\epsilon_1$  and  $\epsilon_2$  have been omitted for simplicity purpose only. Here  $n$  and  $k$  are the real and imaginary part of complex refractive index of metal  $\tilde{n}_m$ , while  $\epsilon_1$  and  $\epsilon_2$  are the real and imaginary part of complex dielectric constant (permittivity) of metal  $\tilde{\epsilon}_m$ . If the propagating electric field is represented by  $E = E_0 e^{i(kz - \omega t)}$ , where  $\kappa = \frac{\tilde{n}_m \omega}{c}$ . The power flowing through the composite structure would be then  $I = |E| \times |E^*| \propto I_0 e^{-\alpha z}$ , where  $\alpha = \frac{2k\omega}{c}$  is the absorption coefficient and it means that  $\alpha \propto k$  (imaginary part of the refractive index of metal). It can be easily set up the relation between  $\epsilon_1 = n^2 - k^2 = 1 - \frac{\lambda^2\lambda_c^2}{(\lambda_p^2\lambda_c^2 + \lambda_p^2\lambda^2)}$  and  $\epsilon_2 = 2nk = \frac{\lambda^3\lambda_c}{(\lambda_p^2\lambda_c^2 + \lambda_p^2\lambda^2)}$ . After some trivial

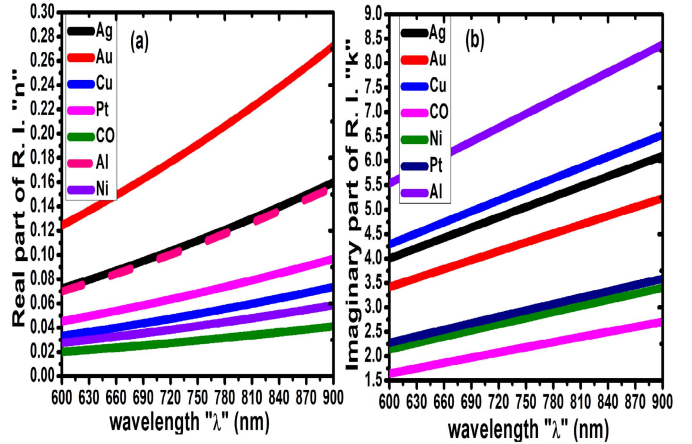


Fig. 3. a) Change of real part of refractive index versus  $\lambda$  (nm) and b) corresponding imaginary part of refractive index of different metals under consideration in this paper.

mathematical manipulation, it can be derived that

$$n = \sqrt{\frac{\epsilon_1 \pm \sqrt{\epsilon_1^2 + \epsilon_2^2}}{2}} \quad (10)$$

$$k = \frac{\epsilon_2}{2\sqrt{\frac{\epsilon_1 \pm \sqrt{\epsilon_1^2 + \epsilon_2^2}}{2}}} \quad (11)$$

eq. (10) and eq. (11) have been simulated for the various metals with the help of eq. (9) and Table-I as reveals in Fig. 3. It is apparent from Fig. 3(a) that the real part of refractive index of various metals obey the following sequence  $\text{Au} > \text{Ag} > \text{Al} > \text{Pt} > \text{Cu} > \text{Ni} > \text{Co}$ . It also increases with wavelength, however this increment is slow for Co metal and fast for Au metal. Also Ag and Al have a very close values of real part of refractive index. Fig. 3(b) reveals the variation of imaginary part of refractive index versus wavelength for various metals, which obeys the following sequence  $\text{Al} > \text{Cu} > \text{Ag} > \text{Au} > \text{Pt} > \text{Ni} > \text{Co}$ . It means Al shows the highest variation and Co shows the minimum variation. Since the absorption coefficient  $\alpha \propto k$ , hence Al is highly absorbent and Co is low absorbent for this present study. Some authors have used the buffer biochemical layer in between of blood sample and metal thin film to avoid direct contact of blood sample with metal, however this buffer layer would reduce the penetration depth of evanescent field to the blood sample for the case of short range of plasmon excitation [1]. It is to be pointed out that by adding buffer layer over thin metal film would rather change the results of computation marginally. Hence the third layer is a buffer layer of constant refractive index  $n_b = 1.45$ . Finally fourth layer is a sensing layer which require only few drops of blood sample due to large optical activity of surface plasmon wave. Hence in this paper only four layer model is considered for basic understanding of surface plasmon resonance excitation condition of different metals. Fig. 1(a) reveals that p-polarized light is incident on prism/metal interface and reflected light from multilayer structure is then collected by detector. Reflectivity has been computed by TMM method as depicted in Fig. 1(b) for this N-layer structure with thickness of each layer  $d_k = z_k - z_{k-1}$ ,

refractive index  $n_k$ , dielectric permittivity  $\epsilon_k$  and permeability  $\mu_k$ . Here the wavelength dependency of each parameter has been removed for the convenience. The tangential components of electric and magnetic fields must be matched at first entry point  $z_1 = 0$  (electric field  $U_1$  and magnetic field  $V_1$ ) and final leaving point  $z = z_{N-1}$  (electric field  $U_N$  and magnetic field  $V_N$ ) by

$$\begin{bmatrix} U_1 \\ V_1 \end{bmatrix} = \prod_{k=2}^{N-1} M_k \begin{bmatrix} U_{N-1} \\ V_{N-1} \end{bmatrix} \quad (12)$$

with

$$M_k = \begin{bmatrix} \cos(\beta_k) & \frac{-i\sin(\beta_k)}{q_k} \\ -iq_k\sin(\beta_k) & \cos(\beta_k) \end{bmatrix} \quad (13)$$

where  $\beta_k = \frac{2\pi}{\lambda} \tilde{n}_k \cos(\theta_k) d_k = \frac{2\pi d_k}{\lambda} \sqrt{\tilde{\epsilon}_k - \tilde{n}_1^2 \sin^2(\theta_i)}$  and  $q_k = \sqrt{\frac{\tilde{\epsilon}_k}{\epsilon_k}} \cos(\theta_k) = \frac{\sqrt{\tilde{\epsilon}_k - \tilde{n}_1^2 \sin^2(\theta_i)}}{\tilde{\epsilon}_k}$ . For the present case  $N = 4$  and  $\tilde{n}_1 = \sqrt{\tilde{\epsilon}_1} = n_p$ ,  $\tilde{n}_2 = \sqrt{\tilde{\epsilon}_m} = \sqrt{\tilde{\epsilon}_2} = \tilde{n}_m$ ,  $\tilde{n}_3 = \sqrt{\tilde{\epsilon}_3} = n_b$  and  $\tilde{n}_4 = \sqrt{\tilde{\epsilon}_4} = n_s|_i$  are the refractive index of prism, metal, buffer and sensing layer (i.e. experimental value of different blood samples) respectively. Also for all the cases  $\mu_k = \mu_0$ , where  $\mu_0$  is the free space permeability. For the present study  $d_1 = 50$  nm is the optimized thickness of concern metal layer,  $d_2 = 20$  nm is the thickness of buffer layer, where  $\theta_i$  is the angle of incident with normal to the axis of prism as depicted in Fig. 1(a). The reflectivity  $R_p = |r_p|^2$  for p-polarized light is given as follow

$$R_p = \left| \frac{(M_{11} + M_{12}q_N)q_1 - (M_{21} + M_{22}q_N)}{(M_{11} + M_{12}q_N)q_1 + (M_{21} + M_{22}q_N)} \right|^2 \quad (14)$$

which has been numerically computed by using TMM technique.

### III. POSSIBILITY OF POWER COUPLING VIA DIFFERENT PRISMS AND OPTIMUM DESIGN

Silica (fused  $\text{SiO}_2$ ) substrate based SPR sensors is quite established technology and required a high attention in next generation sensing technology. However, silica substrate based SPR sensor do not work in infrared (IR) wavelength region. Infact SPR senor working in IR region has a certain advantage such as accurate determination of SPR dip and high probe depth. Infact to shift the SPR resonance dip into IR region essentially required the high refractive index glass or substrate along with precisely matched boundary conditions at the metal-dielectric interface. Fig. 4(a) reveals the refractive index variation of Si, BK7, SF11, 2S2G, LINBO<sub>3</sub> and  $\text{SiO}_2$  prism versus wavelength as their mathematical relations are given in section-II. In this same graph, the refractive index variation of blood groups "O", "A" and "B" have been plotted as per the eq. (2). These graphs have been plotted together to understand whether the SPR condition (i.e.  $n_p > n_s|_i$ ) is fulfilled or not, where  $n_p$  stands for refractive index of selected prism and  $n_s|_i$  stands for refractive index of blood sample. Apparently for any cases of prism  $n_p > n_s|_i$  hence light will be coupled to surface plasmon wave for a given wavelength range, however to excite the surface plasmon in IR region chalcogenide (2S2G), LINBO<sub>3</sub> and Si glasses are most suitable candidates. Since

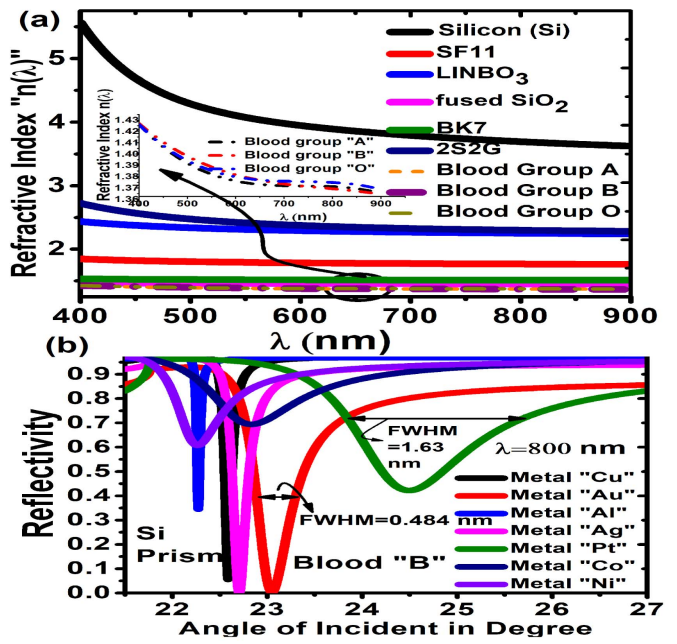
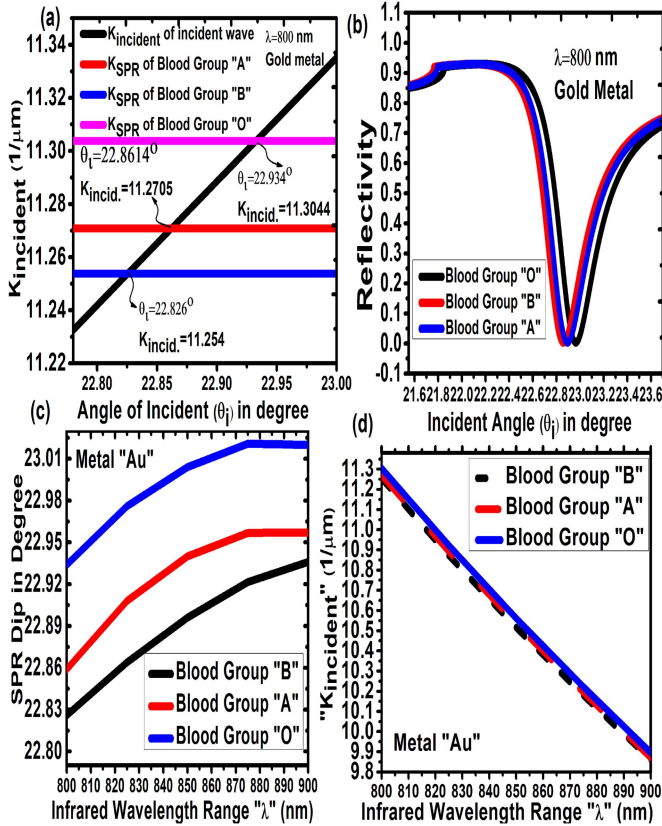


Fig. 4. a) Change of Refractive index with  $\lambda$  (nm) of different glass prisms and blood samples "O", "A" and "B" [5]–[7]. b) Reflectivity versus angle of incident plot for various metal choices.

for the case of Si,  $n_p$  is much greater than  $n_s|_i$  as compared to 2S2G and LINBO<sub>3</sub>, hence the light coupling to surface plasmon would be more prominent in IR region. It means that blood group measurement would be much more successful for the case of Si glass substrate or prism. Fig. 4(b) shows the variation of reflectivity spectrum computed from TMM method for the case of silicon prism and blood sample "B" with different metal choices having  $d_1 = 50$  nm and  $d_2 = 0$  nm at  $\lambda = 800$  nm. It is apparent that FWHM is minimum for the case of Al metal and maximum for the case of Pt metal. Furthermore, lab on a single Si chip can be easily realized due to the recent advancement of Si-based microfluid system and micro-nano-fabrication technology. In continuation to this discussion it is important to know whether the SPR condition of eq. (1) is satisfied or not for the present study. Graphical technique is very efficient way in this regards as reveals in Fig. 5(a), where Au film with thickness of  $d_1 = 50$  nm and Silicon (Si) prism are chosen for the present simulation. It is apparent that  $K_{SPR}$  plots of "O", "B" and "A" blood group cuts the  $K_{incident}$  plot at  $22.934^\circ$ ,  $22.826^\circ$  and  $22.8614^\circ$  resonance angles. In order to validate this results from TMM method, eq. (14) has been simulated to the reflectivity analysis for the same SPR design parameters as in Fig. 5(a). Fig. 5(b) shows the results of TMM method while the SPR angles are  $22.968^\circ$ ,  $22.857^\circ$  and  $22.8936^\circ$  respectively for "O", "B" and "A" blood samples. It means that graphical method results are very closely matched with TMM method. It means that the difference of resonance angle is substantially differ by a factor  $0.111^\circ$ . It has been found that SPR resonance condition is perfectly satisfied for all the other metals too under consideration e.g. Cu, Al, Ag, Pt, Co and Ni but did not present here in this paper for the ease of simplicity. In Fig. 5(b), FWHM are computed to be  $\approx 0.43^\circ$ ,  $\approx 0.47^\circ$  and  $\approx 0.48^\circ$  for A, B and O blood samples respectively at  $\lambda = 800$  nm. Fig. 5(c) shows the



**Fig. 5.** a) Change of incident wave propagation constant ( $K_{\text{incident}}$ ) and SPR wave propagation constant ( $K_{\text{SPR}}$ ) of blood samples "O", "A" and "B" versus angle of incident by using Graphical procedure with buffer layer thickness  $d_2 = 0 \text{ nm}$ . b) Reflectivity computed by transfer matrix method (TMM) approach for the same simulation parameters as Fig. 5(a). Variation of c) SPR resonance dip and d) allowed value of incident wavevector  $K_{\text{incident}}$  in near infrared wavelength range for the case of Au metal.

variation of SPR resonance dip of all the three blood samples in near infrared wavelength range. This plot corresponds to Si prism, with optimum gold thin film thickness  $d_1 = 50 \text{ nm}$  but without buffer layer  $d_2 = 0 \text{ nm}$ . It is apparent from the plot that there is a significant difference of resonance angle which is  $\approx 0.108^\circ$  at  $\lambda = 800 \text{ nm}$  between blood group "O" with blood group "B". However this difference is only  $\approx 0.034^\circ$  between blood group "A" and "B". Fig. 5(d) reveals the variation of allowed incident wavevector  $K_{\text{incident}}$  for the present case in near IR band for all three blood samples. It is apparent from Fig. 2 that the refractive index relation of blood samples has to obey the order as  $n_s|_O > n_s|_A > n_s|_B$  in IR range ( $800 \text{ nm} \leq \lambda \leq 900 \text{ nm}$ ). Hence the blood sample "O" shows the large deviation in terms of SPR dip and  $K_{\text{incident}}$  wavevector parameters as compared to others. This feature is also apparent from Fig. 7 and Fig. 9. It also means that power is much more guided and confined to plasmon mode for the case of blood sample "O".

#### IV. RESULTS OF BLOOD GROUP IDENTIFICATION ANALYSIS OF DIFFERENT METALS IN NEAR INFRARED WAVELENGTH RANGE

Since IR wavelength range (IR-A) has start from 800 nm onwards and experimental values of blood refractive index are

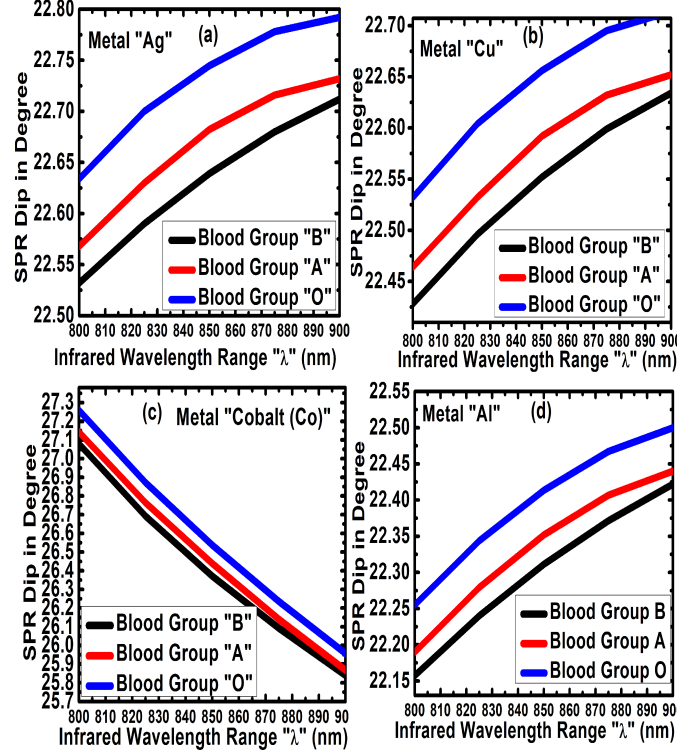


**Fig. 6.** Variation of SPR resonance dip angle versus IR wavelength for the case of different metal choices viz. a) Ag, b) Cu, c) Co and d) Al respectively.

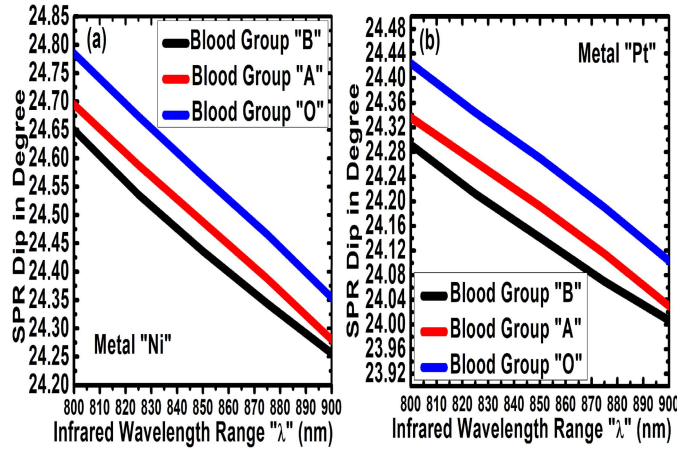


**Fig. 7.** Variation of SPR resonance dip angle in near IR wavelength range for the case of metal choices viz. a) Ni and b) Pt respectively.

available only in wavelength range 400 nm-900 nm. Hence the results of metal selection and analysis are presented only in 800 nm-900 nm wavelength range. Fig. 6 (a, b, c & d) and Fig. 7(a & b) shows the results of variation of SPR dip position in near IR range for metals viz. Ag, Cu, Co, Al, Ni and Pt respectively while  $d_1 = 50 \text{ nm}$  and  $d_2 = 0 \text{ nm}$ . Position of SPR dip increased with wavelength for all metals viz. Ag, Cu, Al except Co, Ni and Pt. It has been found that the difference of SPR dip angle among all the three samples are significant for the case of Co metal with respect to other metals. Apparently higher value of SPR dip angle is attributed to higher  $K_{\text{incident}}$  wavevector. Slope of each curve

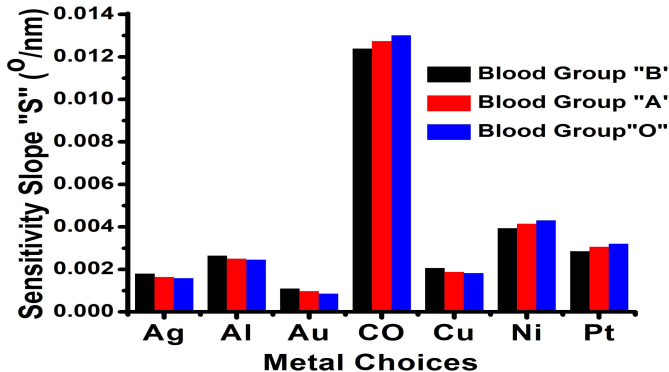


Fig. 8. Sensitivity slope "S" ( $^{\circ}/\text{nm}$ ) of different metal choices viz, Ag, Al, Au, Co, Cu, Ni and Pt for "B", "A" and "O" blood samples.

of Fig. 5(c), Fig. 6 and Fig. 7 reflects the variation of SPR dip with change of IR wavelength, which is defined by sensitivity slope as follow

$$S = \frac{\delta\theta_{SPR}}{\delta\lambda} (^{\circ}/\text{nm}) \quad (15)$$

where the wavelength is measured in nm and superscript  $^{\circ}$  represents the angle in degree. Sensitivity slope is one of the important criteria to achieve an incredibly very high performance of SPR biosensor in IR region. Fig. 8 reveals the sensitivity slope plot for the present cases. It is found to be high  $0.01239 ^{\circ}/\text{nm}$  (blood sample-B),  $0.01274 ^{\circ}/\text{nm}$  (blood sample-A) and  $0.01301 ^{\circ}/\text{nm}$  (blood sample-O) for the case of Co metal. Also, discrimination factor among different blood samples are the highest for the case of Co metal as compared to others. It is also apparent from this plot that Au has a minimum sensitivity slope  $0.0011 ^{\circ}/\text{nm}$ ,  $0.00098 ^{\circ}/\text{nm}$  and  $0.00086 ^{\circ}/\text{nm}$  for blood samples "B", "A" and "O" respectively. Fig. 9 shows the variation of allowed incident wave propagation constant ( $K_{\text{incident}}$ ) of different blood samples "O", "A" and "B" in IR wavelength range for the case of different metal choices. It is found that the  $K_{\text{incident}}$  wavevector decreases with increasing the wavelength for all the metals concern. It has been found that Co has a highest  $K_{\text{incident}}$  wavevector  $13.206 \frac{1}{\mu\text{m}}$  (blood sample "B"),  $13.2344 \frac{1}{\mu\text{m}}$  (blood sample "A"),  $13.287 \frac{1}{\mu\text{m}}$  (blood sample "O") and Al has a lowest  $K_{\text{incident}}$  wavevector  $10.9413 \frac{1}{\mu\text{m}}$  (blood sample B),  $10.9565 \frac{1}{\mu\text{m}}$  (blood sample A),  $10.987 \frac{1}{\mu\text{m}}$  (blood sample O) respectively at  $800 \text{ nm}$ . This feature is attributed to the property that Co has a lowest real and imaginary part of refractive index and Al has a highest imaginary part of refractive index. It means for better blood group discrimination factor the low imaginary part of refractive index of metal is preferred over high imaginary part of refractive index. This is one of the thumb rule of appropriate metal selection for high sensitivity detection of different blood groups. In IR wavelength range  $800 \text{ nm} \leq \lambda \leq 900 \text{ nm}$  incident allowed wavevector follow the following relation  $K_{\text{incident}}|_{\text{sample "O"}} > K_{\text{incident}}|_{\text{sample "A"}} > K_{\text{incident}}|_{\text{sample "B"}}$  due to the different refractive index relation of each blood samples as depicted in Fig. 2. It has been found that  $K_{\text{incident}}|_{\text{Co}} > K_{\text{incident}}|_{\text{Ni}} > K_{\text{incident}}|_{\text{Pt}} > K_{\text{incident}}|_{\text{Au}} > K_{\text{incident}}|_{\text{Ag}} > K_{\text{incident}}|_{\text{Cu}} >$

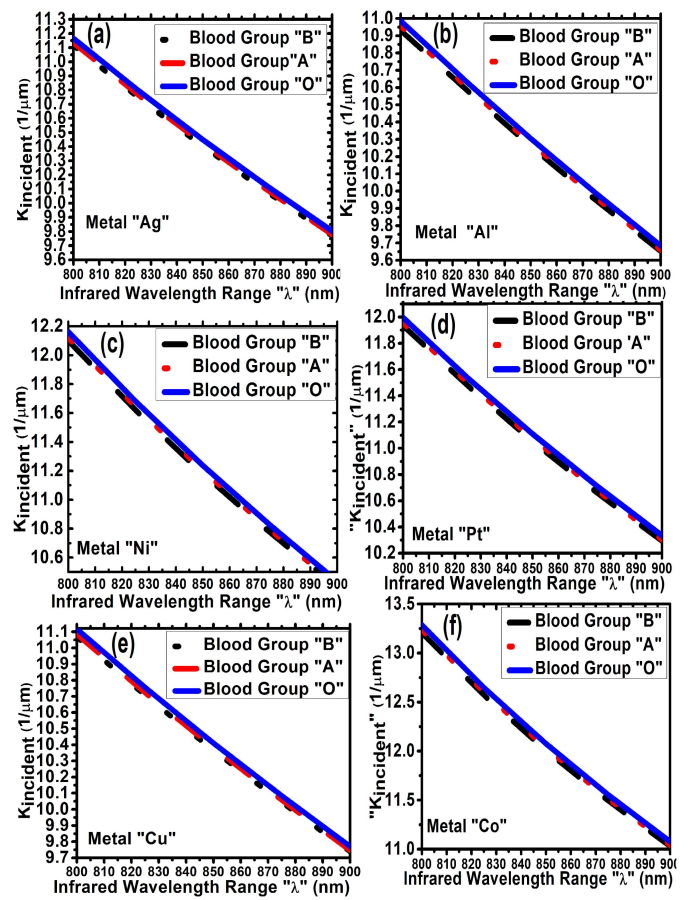


Fig. 9. Variation of allowed incident wave propagation constant ( $K_{\text{incident}}$ ) of different blood samples "O", "A" and "B" versus IR wavelength range for the case of different metal choices viz. a) Ag, b) Al, c) Ni, d) Pt, e) Cu and f) Co respectively. For all the these cases  $d_1 = 50 \text{ nm}$ ,  $d_2 = 0 \text{ nm}$  and Si prism have been considered.

$K_{\text{incident}}|_{\text{Al}}$  for all blood groups and wavelength range of interest due their wavelength dependency of refractive index. Having studied of SPR dip ( $\theta_{SPR}$ ) and  $K_{\text{incident}}$  wavevector position in near IR wavelength range of various metals, one important parameter of SPR biosensor "Blood group discrimination factor" is need to address further. Here we define the blood group discrimination factor  $\delta\theta_{SPR}$  (in  $^{\circ}$ ) which could have three possible values as follow

$$\delta\theta_{SPR}|_{O-A} = |(\theta_{SPR}|_O - \theta_{SPR}|_A)| \quad (16)$$

$$\delta\theta_{SPR}|_{O-B} = |(\theta_{SPR}|_O - \theta_{SPR}|_B)| \quad (17)$$

$$\delta\theta_{SPR}|_{A-B} = |(\theta_{SPR}|_A - \theta_{SPR}|_B)| \quad (18)$$

where outside brackets bar || stands for absolute value and  $\theta_{SPR}|_{i=O,A,B}$  is the SPR dip of each blood sample at particular wavelength. Fig. 10(a, b, c, d, e & f) and Fig. 12(a) shows the results of TMM computation of  $\delta\theta_{SPR}$  to the all above possible cases as in eq. (16-18) for the various metals viz Ag, Al, Pt, Cu, Co, Ni and Au respectively. It has been found that  $\delta\theta_{SPR}|_{O-A}$ ,  $\delta\theta_{SPR}|_{O-B}$  and  $\delta\theta_{SPR}|_{A-B}$  decreases versus IR wavelength range for almost all the metals under consideration in this work. However, this decrement is minimum with Al metal and maximum with Co metal. It is matter of the fact

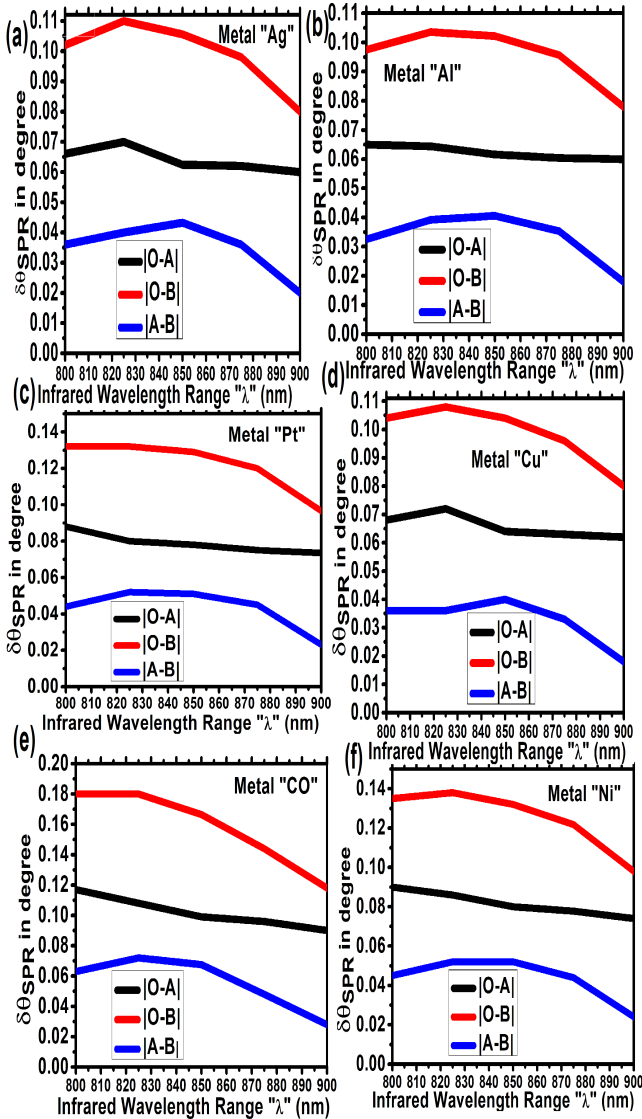


**Fig. 10.** Blood group discrimination factor  $\delta\theta_{SPR} = \theta_{SPR}|_i - \theta_{SPR}|_j$  (where  $i \neq j = O, A, B$  but  $i \neq j$ ) versus IR wavelength for various metals under consideration viz. a) Ag, b) Al, c) Pt, d) Cu, e) Co and f) Ni. For all the these cases  $d_1 = 50$  nm,  $d_2 = 20$  nm (buffer layer) and Si prism have been considered.

that large  $\delta\theta_{SPR}$  would be resultant high precision, accurate and reliable detection of blood samples. It has been found by careful observation of Fig. 10 and Fig. 12(a) that Co metal has a blood group discrimination factor and Al has a minimum as summarized in Tale-II at fix wavelength  $\lambda = 800$  nm. Table-II reveals that Co has a maximum  $\delta\theta_{SPR}$  ( $=0.18^\circ$ ) as compared to traditional Au coated SPR biosensor  $\delta\theta_{SPR}$  ( $=0.108^\circ$ ) [1]. Since modern available commercial detector has an angular resolution as low as  $0.001^\circ$ , hence  $\delta\theta_{SPR}$  for the case of Co metal can be easily detectable for all the three blood samples with quite good precision and reliability. Infact from the Table-II it is apparent that almost all the metals studied in this paper are within the range of angular resolution of modern detector. It can be concluded from this particular study that the choices of the metals should be Co > Ni > Pt > Au > Cu > Ag > Al for the most

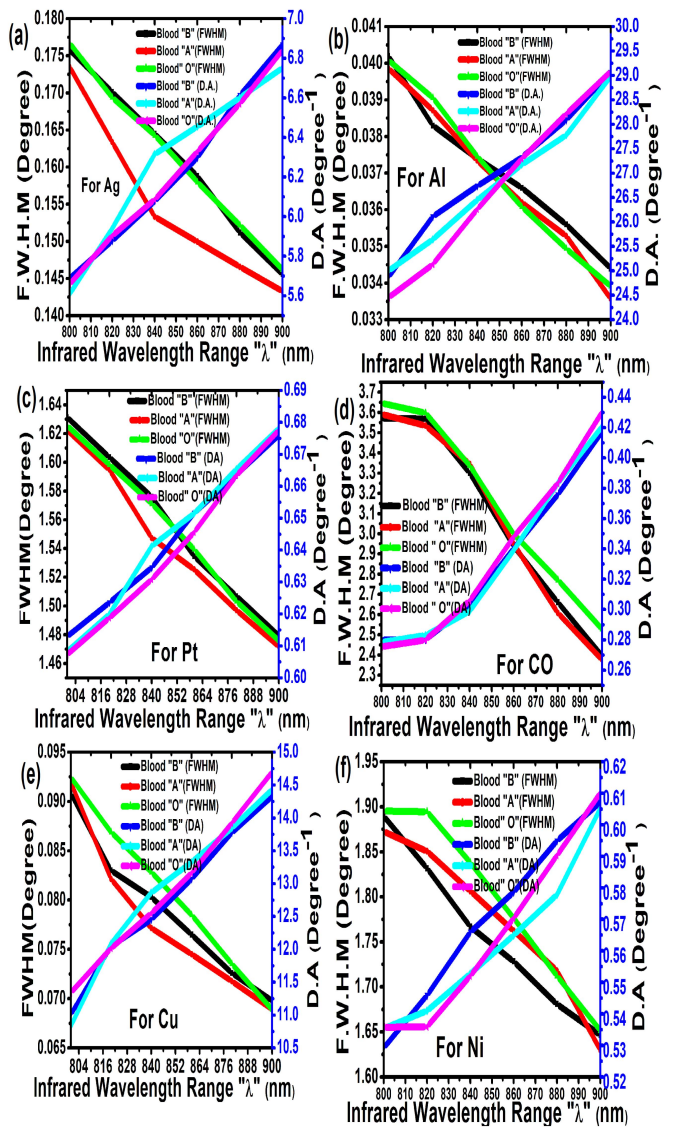


**Fig. 11.** Change of FWHM (in  $^\circ$ ) and corresponding variation of detection accuracy (D.A.) (in  $^\circ$ ) are simultaneously plotted versus IR wavelength for the case of blood groups O, A, B and different metal choices viz. a) Ag, b) Al, c) Pt, d) Co, e) Cu and f) Ni respectively. For all these cases  $d_1 = 50$  nm,  $d_2 = 20$  nm (buffer layer) and Si prism have been considered.

**TABLE II**  
BLOOD GROUP DISCRIMINATION FACTOR  $\delta\theta_{SPR}|_{i-j}$  ( $i \neq j$ ) WHERE  
 $i \neq j = O, A$  AND  $B$  BLOOD GROUPS RESPECTIVELY

Serial no.	Metal	$\delta\theta_{SPR} _{O-A}$ (in $^\circ$ )	$\delta\theta_{SPR} _{O-B}$ (in $^\circ$ )	$\delta\theta_{SPR} _{A-B}$ (in $^\circ$ )
1	Au	0.075	0.108	0.033
2	Ag	0.066	0.102	0.036
3	Cu	0.068	0.104	0.036
4	Al	0.065	0.0975	0.0325
5	Pt	0.088	0.132	0.044
6	Co	0.117	0.18	0.063
7	Ni	0.09	0.135	0.045

reliable and accurate discrimination of blood samples. FWHM decides the sharpness of SPR curves and play a critical role in blood group detection of biosensor. FWHM is defined by

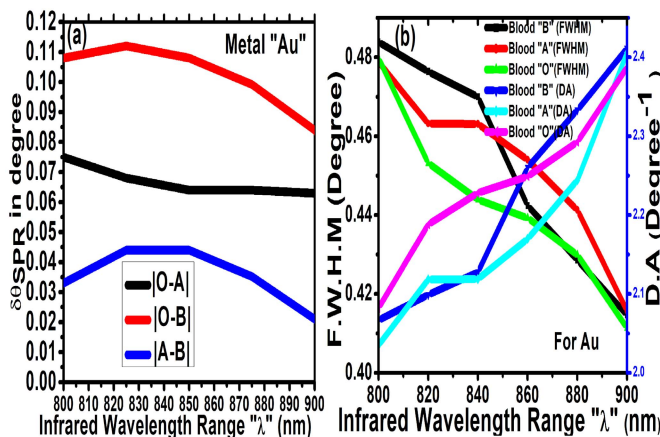


**Fig. 12.** a) Blood group discrimination factor  $\delta\theta_{SPR}$  versus IR wavelength to the case of Au metal for the same simulation parameters as in **Fig. 10**. b) Variation of FWHM (in  $^{\circ}$ ) and D.A. (in  $^{\circ}^{-1}$ ) versus IR wavelength for the case of Au SPR active metal.

TABLE III

DETECTION ACCURACY (D.A.) OF DIFFERENT SPR ACTIVE METALS FOR DIFFERENT BLOOD GROUPS AT  $\lambda = 900$  NM. HERE \* MEANS NOT ABLE TO ESTIMATE

Serial no.	Metal	D.A. (in $^{\circ}^{-1}$ ) Blood "O"	D.A. (in $^{\circ}^{-1}$ ) Blood "A"	D.A. (in $^{\circ}^{-1}$ ) Blood "B"
1	Au	2.4160	2.4155	2.4114
2	Ag	6.8399	6.9589	6.8681
3	Cu	14.2653	14.3678	14.3266
4	Al	28.7356	28.9855	29.0698
5	Pt	*	*	*
6	Co	*	*	*
7	Ni	*	*	*

the width of a line shape at half of its reflectivity spectrum as depicted in **Fig. 4(b)** for some metals. It is argued that  $\delta\theta_{SPR}$  should be high for reliable detection of blood samples, however there is a trade-off between FWHM parameter and  $\delta\theta_{SPR}$ . Apart of large  $\delta\theta_{SPR}$ , FWHM should be as small as possible for better performance of SPR biosensor. Detection accuracy (D.A.) of SPR biosensor is inversely proportional to FWHM ( $D.A. \propto \frac{1}{FWHM}$ ) hence D.A. should be as high as possible. This aspect has been further investigated for optimum choice of SPR active metal with Si prism. Infact if FWHM is too broad then reliability of blood detection will be low. **Fig. 11 (a, b, c, d, e and f)** and **Fig. 12(b)** shows the results of TMM computation of FWHM and D.A. together for all the cases under consideration in this work. It has been found FWHM decreases while D.A. increases with IR wavelength range of interest for all the SPR active metals. It has been found that for the case of active SPR metal like Pt, Co and Ni, FWHM is quite broad and reflectivity spectrum becomes multimode hence difficult to identify the first SPR active mode. **Table-III** shows that results of numerical computation for estimation of FWHM and D.A. of different SPR active metals with Si prism at  $\lambda = 900$  nm,  $d_1 = 50$  nm and  $d_2 = 20$  nm (buffer layer). Infact for the case of Pt, Co, and Ni, D.A. and FWHM could not be detected very precisely due to the disappearance of SPR first active mode at IR wavelength

$\lambda = 900$  nm. It is apparent that D.A. is the highest for the case of Al and Lowest for the case of Au without commenting on metals like Pt, Co and Ni. It can be concluded from this study that the choices of metal should be Al>Cu>Ag>Au for the optimum detection accuracy point of view. After carefully examining the plots and data it has been found that Co has a maximum  $\delta\theta_{SPR}$  but lowest D.A. and Al has a highest D.A. but lowest  $\delta\theta_{SPR}$ . Here the balancing or intermediate value between D.A. and  $\delta\theta_{SPR}$  is required for the optimum choice of metal selection. It can be envisaged that there are pros and cons of each choice of metals. According to **Table-II** and **Table-III** traditional Au based SPR biosensor has average  $\delta\theta_{SPR}|_{i \neq j} = 0.072^{\circ}$  and average D.A.=  $2.4143\frac{1}{\circ}$ . However Ag, Cu, Al, Pt, Co and Ni have average  $\delta\theta_{SPR}|_{i \neq j} = 0.068^{\circ}$ ,  $\delta\theta_{SPR}|_{i \neq j} = 0.0694^{\circ}$ ,  $\delta\theta_{SPR}|_{i \neq j} = 0.065^{\circ}$ ,  $\delta\theta_{SPR}|_{i \neq j} = 0.088^{\circ}$ ,  $\delta\theta_{SPR}|_{i \neq j} = 0.12^{\circ}$  and  $\delta\theta_{SPR}|_{i \neq j} = 0.09^{\circ}$  respectively. Also Ag, Cu and Al have average D.A.=  $6.88\frac{1}{\circ}$ , D.A.=  $14.3199\frac{1}{\circ}$  and D.A.=  $28.9303\frac{1}{\circ}$  respectively. It is evident that Cu has a best intermediate optimum values of  $\delta\theta_{SPR}$  and D.A. while comparing with rest of other SPR active metals. It means that blood discrimination factor  $\delta\theta_{SPR}$  of Al is reduced by a factor of 9.7 % on account of improvement of the detection accuracy (D.A.) by a factor of 91.65 % as compared with traditional Au coated SPR biosensor. Also Cu has D.A.  $\approx$  5.9 times higher than Au based SPR biosensor with almost same blood discrimination factor  $\delta\theta_{SPR}$ . Similary Ag has shown an improvement in D.A.  $\approx$  2.85 times higher with 5.5 % reduction of blood discrimination factor  $\delta\theta_{SPR}$  as compared to traditional Au based SPR biosensor.

## V. CONCLUSION

In this paper blood group identification technique is proposed based on kretschmann configuration of SPR sensor while considering the different seven types of SPR active metals and six types of different substrate prisms. Since buffer layer has been deposited on to SPR active thin metal film, hence oxidization and problem related with direct physical contact of blood sample with SPR active metal is no longer problem in the present study. Actual experimental data of blood samples "O", "A" and "B" have been taken in transfer matrix method (TMM) computation to analyse the pros and cons of different metals and prisms. Performance study of SPR biosensor for blood group detection has been carried out in terms of blood discrimination factor ( $\delta\theta_{SPR}$ ), detection accuracy (D.A.) and sensitivity slope (S). It is important to mention here that Co, Ni and Pt have shown much improved  $\delta\theta_{SPR}$  parameter, however their D.A. could not be claimed due to disappearance of first SPR active mode. It has been found that D.A. for the case of Al, SPR active metal has improved  $\approx$  11.89 times as compared to Au coated SPR biosensor without sacrificing much of  $\delta\theta_{SPR}$  parameter for different blood group identification analysis. However, for the best  $\delta\theta_{SPR}$  parameter point of view, Co has been found to be the best choice. Si prism has been found to be the best choice of substrate material with combination of Al as a SPR active metal for blood group identification. To the best of the authors knowledge this is the first reported study on optimization

problem of SPR active metals and power coupling substrate prisms for blood group identification problems.

## REFERENCES

- [1] R. Jha and A. K. Sharma, "Design of a silicon-based plasmonic biosensor chip for human blood-group identification," *Sens. Actuators B, Chem.*, vol. 145, no. 1, pp. 200–204, Mar. 2010.
- [2] A. K. Sharma, R. Jha, H. S. Pattanaik, and G. J. Mohr, "Design considerations for surface plasmon resonance-based fiber-optic detection of human blood group," *J. Biomed. Opt.*, vol. 14, no. 6, 2009, Art. no. 064041.
- [3] N. Carlie *et al.*, "Measurement of the refractive index dispersion of As<sub>2</sub>Se<sub>3</sub> bulk glass and thin films prior to and after laser irradiation and annealing using prism coupling in the near- and mid-infrared spectral range," *Rev. Sci. Instrum.*, vol. 82, no. 5, May 2011, Art. no. 053103.
- [4] N. L. Kazanskiy, S. N. Khonina, M. A. Butt, A. Kaźmierczak, and R. Piramidowicz, "A numerical investigation of a plasmonic sensor based on a metal-insulator-metal waveguide for simultaneous detection of biological analytes and ambient temperature," *Nanomaterials*, vol. 11, no. 10, p. 2551, Sep. 2021.
- [5] H. Li, L. Lin, and S. Xie, "Refractive index of human whole blood with different types in the visible and near-infrared ranges," *Proc. SPIE*, vol. 3914, pp. 517–521, Jun. 2000.
- [6] R. H. Sagor, M. F. Hassan, S. Sharmin, T. Z. Adry, and M. A. R. Emon, "Numerical investigation of an optimized plasmonic on-chip refractive index sensor for temperature and blood group detection," *Results Phys.*, vol. 19, Dec. 2020, Art. no. 103611.
- [7] R. H. Sagor, M. F. Hassan, A. A. Yaseer, E. Surid, and M. I. Ahmed, "Highly sensitive refractive index sensor optimized for blood group sensing utilizing the Fano resonance," *Appl. Nanoscience*, vol. 11, no. 2, pp. 521–534, Feb. 2021.
- [8] W. Tangkawsakul, T. Srikririn, K. Shinbo, K. Kato, F. Kaneko, and A. Baba, "Application of long-range surface plasmon resonance for ABO blood typing," *Int. J. Anal. Chem.*, vol. 2016, pp. 1–8, Dec. 2016.
- [9] M. Yahya and M. Z. Saghir, "Empirical modelling to predict the refractive index of human blood," *Phys. Med. Biol.*, vol. 61, no. 4, p. 1405, 2016.
- [10] S. Zeng *et al.*, "Graphene–MoS<sub>2</sub> hybrid nanostructures enhanced surface plasmon resonance biosensors," *Sens. Actuators B, Chem.*, vol. 207, pp. 801–810, Feb. 2015.
- [11] S. Patskovsky, A. V. Kabashin, M. Meunier, and J. H. T. Luong, "Near-infrared surface plasmon resonance sensing on a silicon platform," *Sens. Actuators B, Chem.*, vol. 97, nos. 2–3, pp. 409–414, Feb. 2004.
- [12] P. K. Maharana and R. Jha, "Chalcogenide prism and graphene multi-layer based surface plasmon resonance affinity biosensor for high performance," *Sens. Actuators B, Chem.*, vol. 169, pp. 161–166, Jul. 2012.
- [13] D. E. Zelmon, D. L. Small, and D. Jundt, "Infrared corrected sellmeier coefficients for congruently grown lithium niobate and 5 mol.% magnesium oxide-doped lithium niobate," *J. Opt. Soc. Amer. B, Opt. Phys.*, vol. 14, no. 12, pp. 3319–3322, 1997.
- [14] A. K. Mishra and S. K. Mishra, "Infrared SPR sensitivity enhancement using ITO/TiO<sub>2</sub>/silicon overlays," *Europhys. Lett.*, vol. 112, no. 1, p. 10001, Oct. 2015.
- [15] A. K. Mishra, S. K. Mishra, and R. K. Verma, "Graphene and beyond graphene MoS<sub>2</sub>: A new window in surface-plasmon-resonance-based fiber optic sensing," *J. Phys. Chem. C*, vol. 120, no. 5, pp. 2893–2900, Feb. 2016.
- [16] M. A. Ordal *et al.*, "Optical properties of the metals Al, Co, Cu, Au, Fe, Pb, Ni, Pd, Pt, Ag, Ti, and W in the infrared and far infrared," *Appl. Opt.*, vol. 22, no. 7, pp. 1099–1119, 1983.
- [17] M. A. Ordal, R. J. Bell, R. W. Alexander, L. L. Long, and M. R. Querry, "Optical properties of fourteen metals in the infrared and far infrared: Al, Co, Cu, Au, Fe, Pb, Mo, Ni, Pd, Pt, Ag, Ti, V, and W," *Appl. Opt.*, vol. 24, no. 24, pp. 4493–4499, 1985.